J. Phys. D: Appl. Phys. **33** (2000) 2869–2874. Printed in the UK PII: S0022-3727(00)13848-3

# The effect of high-dose nitrogen plasma immersion ion implantation on silicone surfaces

**Imad F Husein†, Chung Chan†, Shu Qin†§ and Paul K Chu‡**

† Plasma Science and Microelectronics Laboratory, Department of Electrical and
Computer Engineering, Northeastern University, Boston, MA 02115, USA
‡ Department of Physics and Materials Science, City University of Hong Kong, 83 Tat Chee,
Kowloon, Hong Kong, People's Republic of China

E-mail: `ihusein@lynx.neu.edu`

Received 10 May 2000

**Abstract.** The effect of plasma immersion ion implantation (PIII) treatment on silicone surfaces was investigated by x-ray photoelectron spectroscopy (XPS), Fourier transform infrared spectroscopy (FTIR-ATR), and scanning electron microscopy (SEM). Low-energy (at voltages of 4 and 8 kV) and high-fluence ($8 \times 10^{17}$ cm$^{-2}$) implantation of nitrogen was performed using an inductively coupled plasma source (ICP) at low pressure (∼0.03 Pa). The IR absorption spectra showed a significant decomposition in the $CH_3$, Si–$CH_3$, and C–F groups of the silicone surface after PIII treatment. The percentage of decomposition was dependent on the implantation energy. The XPS C 1s spectra of the PIII modified surfaces showed an increase in the polar carboxyl (O–C=O) groups and a decrease in the $CF_3$ groups. PIII treatment shifted the XPS Si 2p peak of silicone to a higher binding energy (around 103.2 eV) and the N 1s peak to lower binding energy (around 398.5 eV). The modified Si 2p, N 1s, and O 1s spectra suggest the formation of $SiO_x$ phases, silicon oxynitrides, and silicon nitrides on the silicone surface after PIII treatment.

## 1. Introduction

The modification of the chemical and physical properties of polymer surfaces has been investigated by numerous techniques. The most common treatment methods are wet chemical, ion beams, plasmas, electron beams, UV radiation, $\gamma$ rays, and laser irradiation [1–6]. These techniques have been used to modify the surface chemical structure, energy, hardness, crosslinking, roughness, hydrophobicity, lubricity, conductivity, and biocompatibility of many polymers [4–8]. This article investigates the structural changes in silicone surfaces after treatment by the plasma immersion ion implantation (PIII) technique. PIII combines the characteristics of the ion beam implantation technique and the low-pressure plasma treatment technique.

The PIII technique, also called plasma source ion implantation (PSII) or plasma ion implantation (PII), is a relatively new method for the surface modification of materials. It was first introduced by Conrad *et al* [9] for the modification of metal surfaces. In recent years, the PIII technique has been used in semiconductor processing applications with promising results in shallow junction formation, polycrystalline silicon thin-film transistors hydrogenation, and the formation of silicon on insulator materials [10, 11]. In the PIII treatment, the sample to be treated is immersed in a plasma that is usually maintained at low pressure (between 0.03 and 1 Pa) and plasma densities between $10^8$ and $10^{11}$ ions cm$^{-3}$. Then a series of negative high-voltage pulses (typically a few volts to 300 kV) are applied to the sample. The plasma ions are accelerated across the surrounding sheath and are implanted into the sample surface.

Ion beam modification of polymer materials has been investigated with energies ranging from 50 keV to 10 MeV [2, 12, 13]. Changes in the wettability and chemical structure of silicone rubber using 50–150 keV beams was reported by Suzuki *et al* [14, 15]. Their x-ray photoelectron spectroscopy (XPS) measurements showed no change in the binding energies of the O 1s, C 1s, and Si 2p spectra [14]. This is not in agreement with the XPS results reported in this paper for the PIII modified silicone surfaces. The PIII technique also offers many attractive features over the conventional beam implantation method [10]. Large areas and three-dimensional objects can be processed by PIII at rate orders of magnitude faster than by conventional implantation and without the need for sample manipulation. In addition, in applications requiring low-energy implantation (less than 10 keV) and high doses, the conventional ion beam technique is limited by the focusing optics [10, 11].

Plasma treatment of polymer surfaces is more complex in nature than the ion beam implantation technique. The effect

---

§ Current address: Silicon Genesis Corporation, Bedford, MA 01730, USA.

0022-3727/00/222869+06$30.00

of the interaction of the plasma ions (10–30 eV) with the surface is only one piece of the puzzle [16]. Plasma electrons (1–10 eV), UV, and vacuum UV also contribute to the modification process [3, 16]. The processing pressure is usually between 40 and $10^3$ Pa, which is higher than the processing pressure used in this study ($\sim$0.03 Pa). Morra *et al* investigated the hydrophobic recovery of oxygen plasma treated polydimethylsiloxane (PDMS) surfaces [17]. The mechanisms of hydrophobic recovery of plasma treated PDMS were addressed by Owens and Smith [18]. Everaert *et al* showed that the aging of plasma treated silicone rubber can be slowed down by repeating the plasma treatment [19].

Recently, we showed that PIII treatment of silicone and EPDM at high doses reduced the surface coefficient of friction considerably [20]. In this paper, the effects of high-dose and low-energy implantation of nitrogen on the surface chemistry and surface morphology of silicone are investigated. The surfaces are characterized by XPS, attenuated total reflectance Fourier transform infrared spectroscopy (FTIR-ATR), scanning electron miroscopy (SEM), and roughness measurement.

## 2. Experiment

Silicone rubber sheets (L-13430), provided by Acushnet Rubber Company, Inc. (New Bedford, MA), were cut into $5 \times 6.4 \times 0.16$ cm$^3$ pieces and cleaned by iso propyl alcohol and then washed by distilled water prior to the PIII treatment. The samples were treated in an inductively-coupled plasma system where the plasma is generated by a planar antenna coil placed on top of a fused quartz window outside the vacuum chamber. The coil is connected in series with a capacitive matching network to the radio frequency (RF) input. A detailed description and illustration of this system can be found in [10]. The samples were processed under the following conditions: base pressure $= 8 \times 10^{-4}$ Pa ($6 \times 10^{-6}$ Torr), processing pressure $\sim$0.03 Pa (0.2 mTorr), RF power = 430 W, and plasma density of $\sim 6 \times 10^{10}$ cm$^{-3}$. The plasma ions were accelerated by applying negative voltage pulses of $-4$ and $-8$ kV with pulse widths of 8 $\mu$s and repetition frequencies of 2 kHz to the sample holder. The samples were treated for 45 min to achieve an approximate dose of $8 \times 10^{17}$ cm$^{-2}$ [10]. The sample holder temperature was maintained at around 30 °C by cooling it during the treatment.

In PIII, the incident ions have a distribution of energies. A fraction of the ions (typically 10–30%) are implanted at energies that are less than the magnitude of the applied voltage. Low-energy ions are implanted during the finite rise and fall time of the voltage pulse [10]. This results in a higher concentration of the implanted ion species at the surface compared with the conventional ion beam methods. Also, in the case of nitrogen plasma, atomic nitrogen ions ($N^+$) and molecular ions ($N_2^+$) are incident on the surface (mostly $N_2^+$ under the above experimental conditions). This produces broader implant profiles than those of conventional implantation due to the varied stopping ranges of $N^+$ and $N_2^+$. The projected range distribution of $N_2^+$ and $N^+$ in silicone can be estimated using transport of ions in matter (TRIM) simulation (version SRIM 2000) [21]. Simulations for the stopping of 8 keV $N^+$ and $N_2^+$ ions in silicone produced projected ranges of 31.4 and 19.7 nm with straggling of 13.2 and 7.3 nm, respectively. While the projected ranges for 4 keV $N^+$ and $N_2^+$ in silicone are 17 and 11.6 nm with straggling of 7.8 and 4.6 nm, respectively.

The chemical composition and the nature of the chemical bonds were determined by FTIR-ATR and XPS analysis of the survey scans and high-resolution spectra of the Si 2p, O 1s, C 1s, and N 1s lines. XPS spectra were obtained with a Physical Electronics model 5500MT ESCA instrument at a base pressure of $5 \times 10^{-10}$ Torr using a monochromated Al K$\alpha$ 1486.6 eV source. A low-energy electron flood gun was used to neutralize sample charging. The take off and acceptance angles were 65° and ±7°, respectively. Survey scans were obtained using a pass energy of 117.4 eV and covering 800 $\mu$m diameter analysis area. High-resolution scans of the C 1s, O 1s, N 1s, Si 2p lines were obtained using a pass energy of 58.7 eV. Binding energies were determined by setting the binding energy of C–C and C–H bonds to 284.75 eV. Estimates of the relative amounts of carbon binding states were obtained through nonlinear least squares fitting of the C 1s spectra.

The IR spectra were obtained with a Biorad (FTS-45) Fourier transform spectrometer combined with ATR. The incident angle of infrared light against the Ge prism was 45°. The absorbance in the range 600–4000 cm$^{-1}$ was obtained with a spectral resolution of 4 cm$^{-1}$ and 64 scans were recorded on each sample. SEM and surface roughness measurements were used to study the modification of the surface topography. The SEM photographs were obtained using a JEOL JSM-IC848 electron microscope (JEOL, Peabody, MA). The surface profilometry scans and the average surface roughness ($R_a$) were obtained by a Sloan DEKTAK 3030.

## 3. Results and discussion

The FTIR-ATR absorption bands of a silicone surface before and after $N_2$ PIII treatment are shown in figures 1(a)–(c) at wavenumbers ranging from 600 to 1800 cm$^{-1}$. The bands that occur outside this range are the $CH_3$ asymmetric stretch at 2960 cm$^{-1}$, the $CH_3$ symmetric stretch at 2880 cm$^{-1}$, and the OH stretching vibration of SiOH at 3700 cm$^{-1}$ [22–24]. These bands are weak in comparison with the numerous bands in the 600–1800 cm$^{-1}$ absorption ranges and thus are not shown in figure 1. The intense absorption bands around 1020 cm$^{-1}$ (band 1) and 1080 cm$^{-1}$ (band 2) in figure 1(a) are characteristic of the Si–O–Si chain asymmetric stretch in siloxanes [22–24]. Nitrogen implantation at 8 keV deformed the siloxane band at 1080 cm$^{-1}$ and merged it with its sister band at 1020 cm$^{-1}$ (as shown in figure 1(b)) to form a wide band with an asymmetric shape between 1000 and 1200 cm$^{-1}$. This shape of absorption bands is a characteristic of the asymmetric stretch of the Si–O–Si chain in silica [22, 23]. Figure 1(c) shows that nitrogen implantation at a lower energy (4 keV) with the same fluence caused less transformation in the siloxane bonds.

The area of the IR absorption peak is proportional to the concentration of the corresponding bonds. Thus, comparison of the intensities (areas) of the IR absorption peaks for

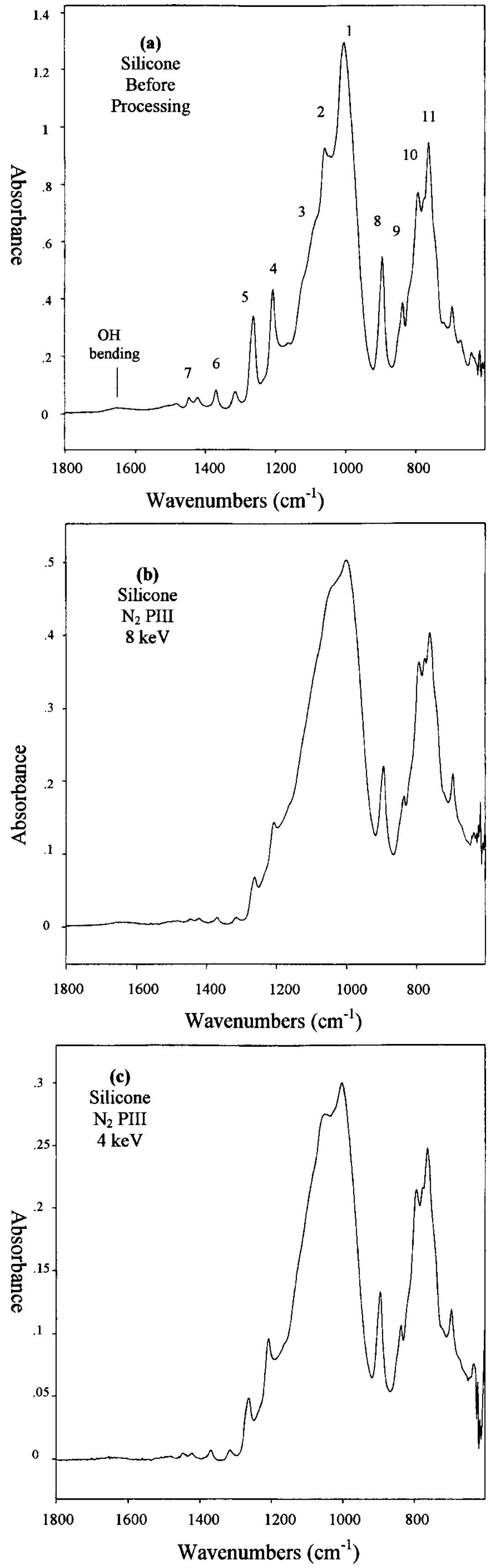

**Figure 1.** FTIR-ATR spectrum of (a) an untreated silicone surface, (b) a PIII modified silicone surface by $N_2$ using 8 kV pulses and (c) a PIII modified silicone surface by $N_2$ using 4 kV pulses. The implantation dose in (b) and (c) is the same.

the untreated silicone surface with the corresponding peak intensities of the PIII modified silicone surfaces in figure 1, will give some insight into the changes in bonding after PIII treatment. The following significant changes were observed. First, the intensity of the absorption band at 1210 $cm^{-1}$ (band 4) which is associated with the C–F asymmetric stretch [23] decreased significantly after 8 keV PIII treatment. This change in intensity can be quantified by approximating the band area (intensity) as the product of the absorbance and the bandwidth at half-absorbance (half-bandwidth) [25]. This method yields absorption-band areas, for the C–F asymmetric stretch band, of 6.08, 2.125, and 0.932 (arbitrary units) for the untreated, the 4 keV implanted, and the 8 keV implanted silicone, respectively. Thus, PIII treatment decomposed a significant number of C–F bonds, especially at higher implantation energies. The C–F symmetric stretch band occurs around 1150 $cm^{-1}$ (band 3) [23] overlapping with the Si–O–Si asymmetric stretch bands and appearing like a shoulder in figure 1(a). This shoulder is not clearly observed in the implanted samples (figures 1(b) and (c)).

The second significant observation about the IR spectrum is the decomposition of methyl ($CH_3$) groups and methyl groups attached to silicon atoms as can be seen by the decrease in the intensity of the absorption bands that are associated with these groups. The intensity of the Si–$CH_3$ symmetric bend (umbrella mode) around 1265 $cm^{-1}$ (band 5) [22] in figure 1(a) decreased approximately by factors of 6 and 2.5 after $N_2$ PIII treatment at 8 and 4 keV, respectively (figures 1(b) and (c)). The $CH_3$ symmetric bend at 1370 $cm^{-1}$ (band 6) and the $CH_3$ asymmetric bend around 1460 $cm^{-1}$ (band 7) also decreased in intensity after $N_2$ PIII [22–24]. The two weak bands observed in the silicone sample spectrum and assigned to the $CH_3$ asymmetric stretch (at 2960 $cm^{-1}$) and the $CH_3$ symmetric stretch (at 2880 $cm^{-1}$) were difficult to observe in the spectra of the PIII modified samples (not shown in figure 1). Also, the Si–$CH_3$ bond shows absorbance at the wavenumbers 845 $cm^{-1}$ (band 9) and 765 $cm^{-1}$ (band 11) which are assigned to the $Si(CH_3)_2$ rocking mode [23, 24].

Silicone surfaces react upon exposure to atmospheric moisture to form silanol bonds (Si–OH) [22, 23]. This is evident in the existence of a small broad band around 1640 $cm^{-1}$ attributed to OH bending as shown in figure 1(a) and the presence of a weak band around 3700 $cm^{-1}$ due to the OH stretching of SiOH (not shown). In previous studies, modification of silicone rubber by plasma [17] and ion beam implantation [14, 15] increased the number of silanol groups. This is not the case in the PIII modified surfaces, as shown in figures 1(b) and (c). The band at around 910 $cm^{-1}$ (band 8) may be related to the Si–O stretch in silanol. But this is difficult to validate in silicones because this band is relatively insensitive to hydrogen bonding [22].

Table 1 shows the XPS survey analysis results of an untreated silicone surface and a $N_2$ implanted silicone surface by PIII at 8 keV. XPS characterization samples a thin surface layer of 10–200 Å, which controls the surface-sensitive properties (e.g. adhesion) [26], while the FTIR-ATR probes a fairly deep surface layer of 0.2–1 $\mu$m. The atomic composition of the PIII modified surface shows an increase in oxygen, silicon, and nitrogen by comparison with the

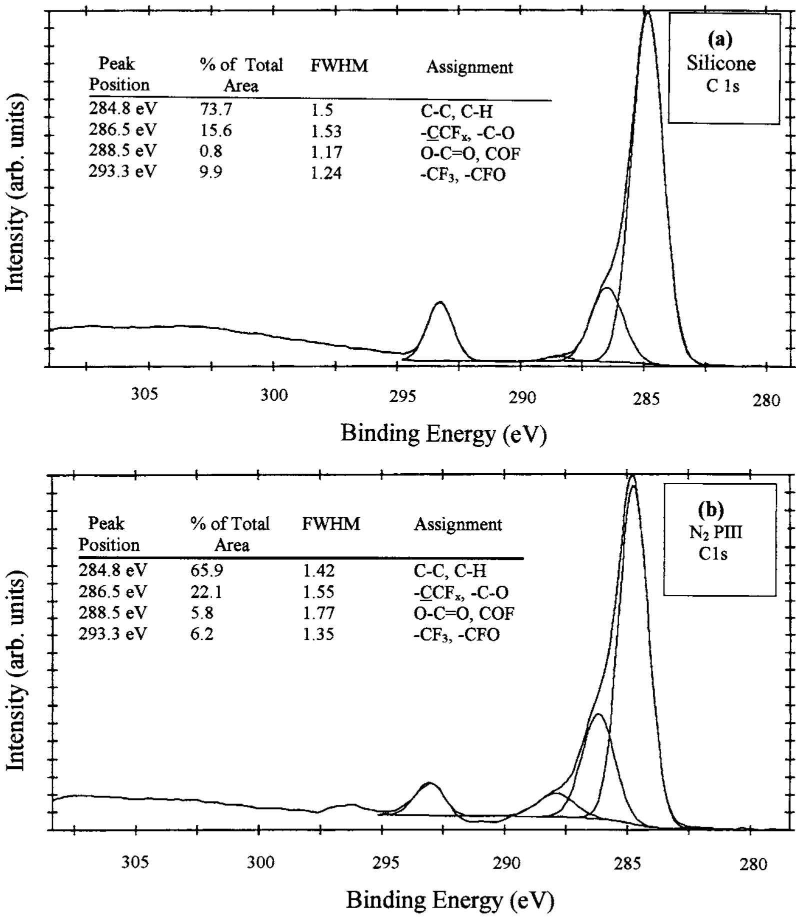

| Peak Position | % of Total Area | FWHM | Assignment |
|---|---|---|---|
| 284.8 eV | 73.7 | 1.5 | C-C, C-H |
| 286.5 eV | 15.6 | 1.53 | -<u>C</u>$CF_x$, -C-O |
| 288.5 eV | 0.8 | 1.17 | O-C=O, COF |
| 293.3 eV | 9.9 | 1.24 | -$CF_3$, -CFO |

| Peak Position | % of Total Area | FWHM | Assignment |
|---|---|---|---|
| 284.8 eV | 65.9 | 1.42 | C-C, C-H |
| 286.5 eV | 22.1 | 1.55 | -<u>C</u>$CF_x$, -C-O |
| 288.5 eV | 5.8 | 1.77 | O-C=O, COF |
| 293.3 eV | 6.2 | 1.35 | -$CF_3$, -CFO |

**Figure 2.** C 1s region of XPS spectra and its deconvolution components of (a) an untreated silicone surface and (b) a PIII modified surface by N2 using 8 kV pulses.

**Table 1.** XPS survey analysis of a silicone surface and a nitrogen modified silicone surface by PIII using 8 kV pulses.

| | Surface composition (at.%) | | | | | |
|---|---|---|---|---|---|---|
| | C | O | Si | N | F | Cl |
| Silicone | 47.8 | 20.0 | 16.8 | 0.4 | 14.5 | 0.2 |
| PIII modified | 29.5 | 39.5 | 20.4 | 3.9 | 4.9 | 0.8 |

untreated surface. This change is accompanied by a decrease in the amount of carbon and fluorine in the implanted sample.

Figure 2 displays the C 1s region of the XPS of unmodified silicone (figure 2(a)) and PIII modified silicone (figure 2(b)). Deconvolution of the C 1s peak reveals the existence of carbon in four chemical states. The following peak assignments are made for the four C 1s peaks: hydrocarbons at 284.8 eV, $CCF_x$/C–O at 286.5 eV, O–C=O/COF at 288.5 eV, and $CF_3$/CFO at 293.3 eV [27, 28]. The percentages of each type of these carbon-binding states are listed in figure 2. The nitrogen implanted sample (figure 2(a)) showed a decrease in the C–C/C–H bonds and the $CF_3$ component. This supports the decrease in the intensity of the IR bands that are associated with $CH_3$ groups and C–F groups. While the area ratio and intensity of the $CCF_x$/C–O and the O–C=O/COF peaks increased after PIII treatment. In particular, the major increase in the hydrophilic O–C=O bond (polar group) from 0.8 to 5.8% after implantation explains our previous results [20] on the increase in the surface energy (decrease in water contact angle) of nitrogen modified silicone surfaces. The decrease in fluorocarbons is also supported by the F 1s spectrum (not shown). In the modified sample, the main F 1s peak was slightly shifted (0.4 eV) toward lower energies and a new peak was formed around 684.5 eV, which is consistent with inorganic fluoride species.

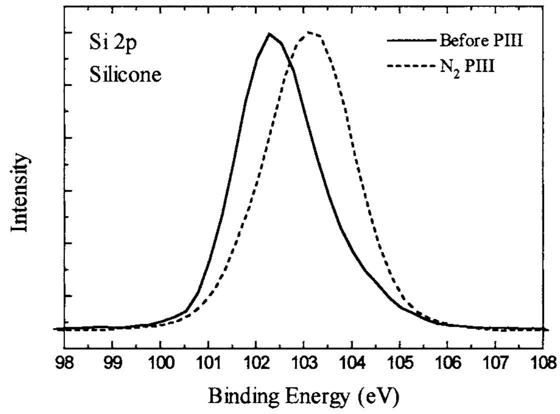

**Figure 3.** XPS spectra of the Si 2p region for an unmodified silicone surface and a PIII modified silicone surface by $N_2$ at 8 kV pulses.

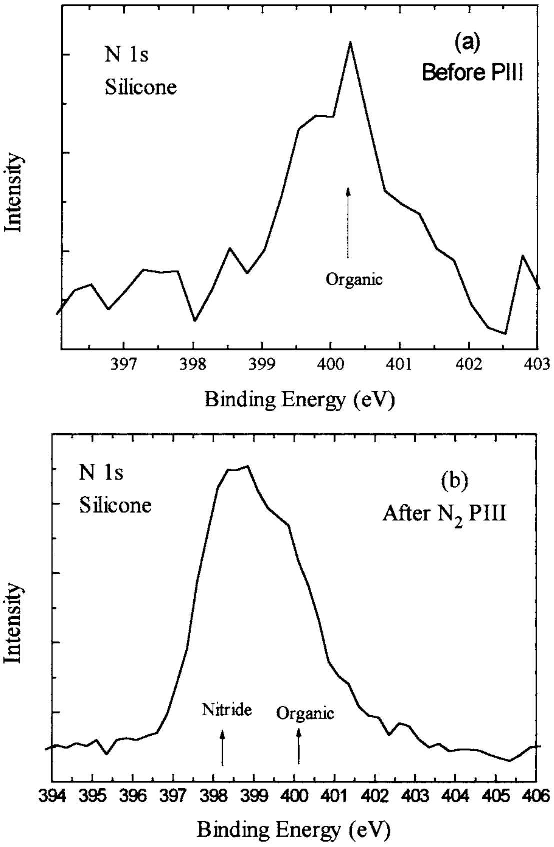

**Figure 4.** XPS spectra of the N 1s region for (a) an unmodified silicone surface and (b) a PIII modified silicone surface by $N_2$ at 8 kV pulses.

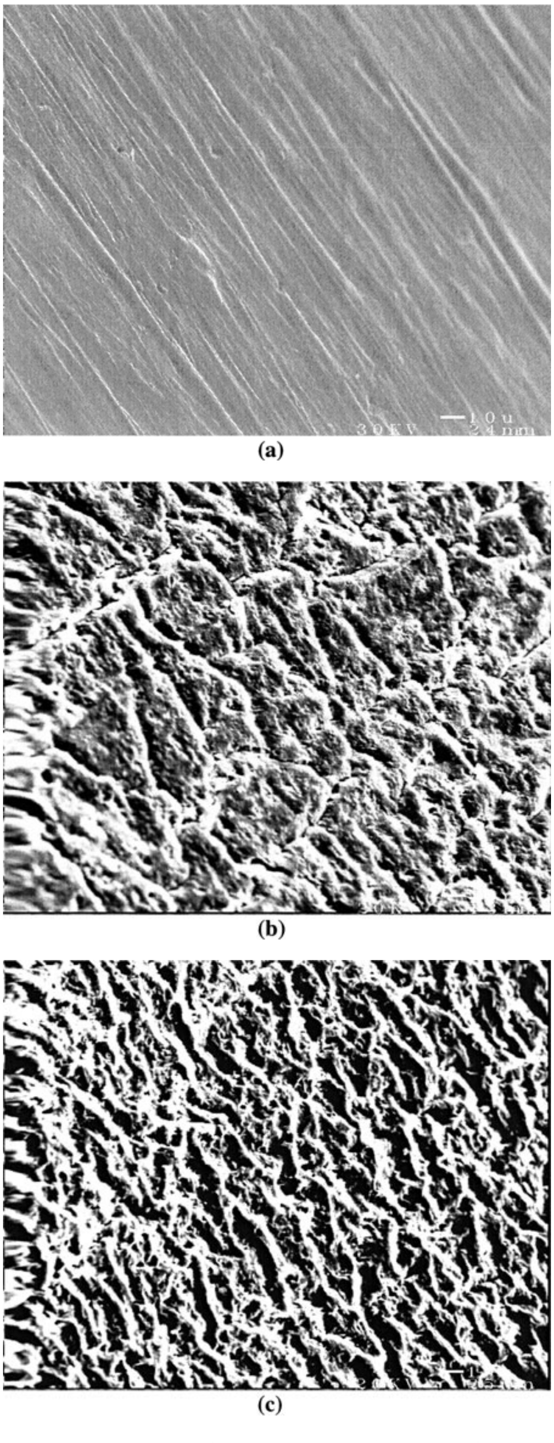

**Figure 5.** SEM images of (a) an untreated silicone surface, (b) a PIII modified silicone surface by $N_2$ at 8 kV pulses and (c) a PIII modified silicone surface by $N_2$ at 4 kV pulses.

The XPS high-resolution spectra of the Si 2p line for a silicone surface and a $N_2$ PIII modified surface are shown in figure 3. The binding energy of the Si 2p peak of the untreated sample is around 102.2 eV, which is consistent with the reported values for silicone [17, 18, 28]. After PIII treatment, the Si 2p peak binding energy is shifted by about 1.0 eV higher (at a B.E. = 103.2 eV). This energy shift is too high to be assigned to organic silicone species and is more consistent with binding energies assigned to $SiO_x$ and $SiO_xN_y$ phases [29, 30]. This supports the FTIR-ATR spectra results which suggested the decomposition of the siloxane bonds in the silicone after PIII treatment. From table 1 the O:Si ratio in the PIII modified sample is 39.5:20.4 ($SiO_{1.94}$). The Si 2p binding energy of this $SiO_x$ phase ($x = 1.94$) should be close to that of the Si 2p binding energy of $SiO_2$, which is around 104.2 eV [29]. But not all the oxygen atoms are attached to silicon (e.g. the C 1s showed the existence of small C–O groups). Therefore, the O:Si ratio in $SiO_x$ should be less than 1.94 and this will cause a shift in the Si 2p peak of $SiO_x$ to lower binding energies [29].

The Si 2p peak at 103.2 eV may also suggest the formation of silicon oxynitrides. The Si 2p binding energy of silicon oxynitrides ($SiO_xN_y$) falls between that of $SiO_2$ at 104.2 eV and silicon nitride ($Si_3N_4$) at 102.8 eV, depending on the Si:O:N ratios [29]. Thus, a silicon oxynitride of a form similar to $SiO_{1.94}N_{0.19}$ (see table 1) will have a Si 2p binding energy between 102.8 and 104.2 eV. Figure 4(a) shows the XPS high-resolution spectrum of a silicone surface for the N 1s region. The peak occurs around a binding energy of 400 eV, which is consistent with the existence of nitrogen in an organic form [28]. The N 1s peak of the PIII modified surface (figure 4(b)) is shifted toward lower binding energies (around 398.5 eV), which indicates the formation of nitrides and oxynitrides such as $SiN_x$ and $SiO_xN_y$ after implantation [29, 30]. Also, the O 1s peak (not shown) of the PIII modified surface occurred at a higher binding energy than that of the untreated silicone surface by about 0.3 eV.

The changes in surface topography after PIII were studied using SEM and roughness measurements. Figures 5(a)–(c) display the SEM photographs obtained for untreated silicone, PIII treated silicone at 8 keV, and PII treated silicone at 4 keV, respectively. The average surface roughness was determined by performing two perpendicular scans on the surface. The untreated sample exhibited average surface roughness valves of 0.664 and 0.275 $\mu$m in two perpendicular directions. PIII modification at low energy (4 keV) created deep valleys in the silicone surface (figure 5(c)) and increased the average surface roughness in both directions to 1.493 and 0.501 $\mu$m. Less surface sputtering occurred during the 8 kV pulses implantation. Average surface roughness values of 0.624 and 0.335 $\mu$m were recorded for this surface.

## 4. Conclusion

The structural effects of nitrogen plasma immersion ion implantation in silicone surfaces were investigated using FTIR-ATR, XPS, and SEM. The FTIR-ATR results showed that PIII treatment caused two major changes. First, a significant decrease in the intensity (area) of the absorption bands that are associated with the organic functional groups attached to the Si atoms. Second, deformation of the siloxane absorption bands at 1020 and 1080 cm$^{-1}$ and the formation of a wide asymmetric band between 1000 and 1200 cm$^{-1}$, especially at higher implantation energies. XPS analysis of the modified surfaces showed an increase in oxygen, silicon, and nitrogen. XPS high-resolution spectra of the Si 2p and N 1s lines indicate the decomposition of the organic silicone species by PIII and the formation of a ceramic-like surface that can be assigned to $SiO_x$, $SiO_xN_y$, and $SiN_x$. PIII treatment increased the hydrophilic O–C=O bond on the surface which contributes to the increase in surface energy.

## Acknowledgments

The authors would like to thank Dr C V Cooper of United Technologies Research Center (East Hartford, CT) for his help in obtaining the roughness measurements, Professor Jeffrey Hopwood for useful discussions and Mr. Joe Jenevich for his help in constructing the experimental apparatus.

## References

[1] Garbassi F, Morra M and Occhiello E 1998 *Polymer Surfaces: From Physics to Technology* (Chichester: Wiley) pp 235–88

[2] Lee E H 1999 *Nucl. Instrum. Methods Phys. Res.* B **151** 29

[3] Wertheimer M R, Fozza A C and Hollander A 1999 *Nucl. Instrum. Methods Phys. Res.* B **151** 65

[4] Chan C-M, Ko T-M and Hiraoka H 1996 *Surf. Sci. Rep.* **24** 1–54

[5] Chan C-M 1994 *Polymer Surface Modification and Characterization* (Cincinnati: Hanser/Gardner)

[6] Chou N J and Chang C-A 1994 *Characterization of Polymers* ed N J Chou *et al* (Stoneham, MA: Butterworth-Heinemann) pp 169–97

[7] Koberstein J T 1996 *MRS Bull.* **21** 19

[8] Coates D M and Kaplan S L 1996 *MRS Bull.* **21** 43

[9] Conrad J R, Radtke J L, Dodd R A and Worzala F J 1987 *J. Appl. Phys.* **62** 4591

[10] Chu P K, Qin S, Chan C, Cheung N W and Larson L A 1996 *Mater. Sci. Eng.* R **17** 207

[11] Mantese J V, Brown I G, Cheung N W and Collins G A 1996 *MRS Bull.* **21** 52

[12] Gerstner E G, McCulloch D G, Mckenzie D R and Yap E 1999 *Phil. Mag.* A **79** 391

[13] Lee E H, Lee Y, Oliver W C and Mansur L K 1993 *J. Mater. Res.* **8** 377

[14] Suzuki Y, Kusakabe M, Iwaki M and Suzuki M 1988 *Nucl. Instrum. Methods Phys. Res.* B **32** 120

[15] Suzuki Y, Swapp C, Kusakabe M and Iwaki M 1990 *Nucl. Instrum. Methods Phys. Res.* B **46** 354

[16] France R M and Short R D 1998 *Langmuir* **14** 4827

[17] Morra M, Occhiello E, Marola R, Garbassi F, Humphrey P and Johnson D 1990 *J. Colloid Interface Sci.* **137** 11

[18] Owens M J and Smith P J 1996 *Polymer Surface Modification: Relevance to Adhesion* ed K L Mittal (Utrecht, The Netherlands: VSP) pp 3–15

[19] Everaert E P, Van Der Mei H C, De Vries J and Busscher H J 1996 *Polymer Surface Modification: Relevance to Adhesion* ed K L Mittal (Utrecht, The Netherlands: VSP) pp 33–48

[20] Husein I F, Zhou Y, Qin S, Chan C, Kleiman J I and Marchev K 1997 *Materials Modification and Synthesis by Ion Beam Processing (MRS Symp. Proc. 438)* ed D E Alexander *et al* (Pittsburgh, PA: MRS) p 511

[21] Ziegler J F, Biersack J B and Littmark U 1985 *The Stopping and Range of Ions in Solids* (New York: Pergamon)

[22] Lipp E D and Smith A L 1991 *The Analytical Chemistry of Silicones* ed A L Smith (New York: Wiley) pp 305–45

[23] Smith B 1999 *Infrared Spectral Interpretation* (Boca Raton, FL: CRC)

[24] Socrates G 1994 *Infrared Characteristic Group Frequencies: Tables and Charts* (Chichester: Wiley)

[25] Lanford W A and Rand M J 1978 *J. Appl. Phys.* **49** 2473

[26] Zhuang H and Gardella J A 1996 *MRS Bull.* **21** 43

[27] Briggs D 1998 *Surface Analysis of Polymers by XPS and Static SIMS* (Cambridge: Cambridge University Press) pp 47–87

[28] Beamson G and Briggs D 1992 *High Resolution XPS of Organic Polymers: The Scienta ESCA300 Database* (Chichester: Wiley)

[29] Strass A, Bieringer P, Hansch W, Fuenzalida V, Alvarez A, Luna J, Martil I, Martinez F L and Eisele I 1999 *Thin Solid Films* **349** 135

[30] Khoueir A, Lu Z H, Ng W T and Ma Y 2000 *J. Vac. Sci. Technol.* A **18** 724